

RESEARCH ARTICLE | JULY 24 2023

Spin- and angle-resolved photoemission spectroscopy study of heptahelicene layers on Cu(111) surfaces

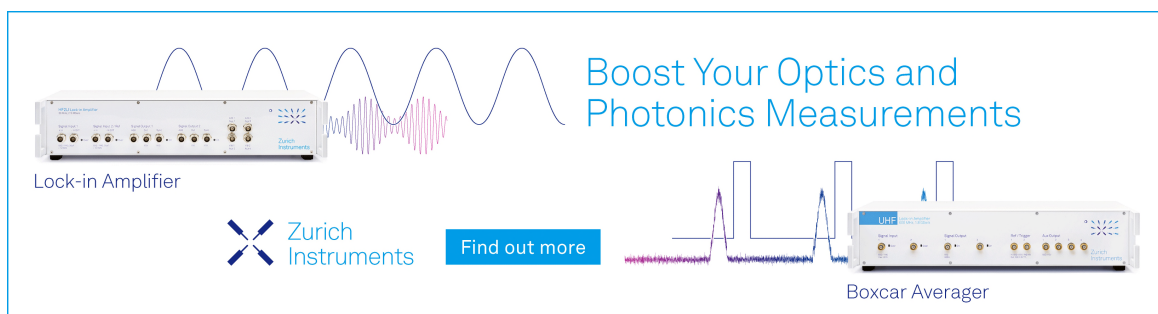
Special Collection: [Chiral Induced Spin Selectivity](#)

M. Baljzović ; B. Arnoldi; S. Grass ; J. Lacour ; M. Aeschlimann ; B. Stadtmüller ; K.-H. Ernst  

 Check for updates


J. Chem. Phys. 159, 044701 (2023)

<https://doi.org/10.1063/5.0156581>



Boost Your Optics and
Photonics Measurements

Lock-in Amplifier

 Zurich
Instruments

[Find out more](#)

Boxcar Averager

Spin- and angle-resolved photoemission spectroscopy study of heptahelicene layers on Cu(111) surfaces

Cite as: J. Chem. Phys. 159, 044701 (2023); doi: 10.1063/5.0156581

Submitted: 1 May 2023 • Accepted: 29 June 2023 •

Published Online: 24 July 2023



View Online



Export Citation



CrossMark

M. Baljović,¹  B. Arnoldi,² S. Grass,³  J. Lacour,³  M. Aeschlimann,²  B. Stadtmüller,^{2,4} 
and K.-H. Ernst^{1,5,6,a)} 

AFFILIATIONS

¹ Molecular Surface Science Group, Empa, Swiss Federal Laboratories for Materials Science and Technology, 8600 Dübendorf, Switzerland

² Department of Physics and Research Center OPTIMAS, Rheinland-Pfälzische Technische Universität (RPTU) Kaiserslautern-Landau, 67663 Kaiserslautern, Germany

³ Department of Organic Chemistry, University of Geneva, 1211 Geneva 4, Switzerland

⁴ Institute of Physics Johannes Gutenberg-University Mainz, 55099 Mainz, Germany

⁵ Nanosurf Laboratory, Institute of Physics, The Czech Academy of Sciences, 16200 Prague, Czech Republic

⁶ Department of Chemistry, University of Zurich, 8057 Zürich, Switzerland

Note: This paper is part of the JCP Special Topic on Chiral Induced Spin Selectivity.

^{a)} **Author to whom correspondence should be addressed:** ernst@fzu.cz

ABSTRACT

It has been demonstrated previously that electrons interact differently with chiral molecules depending on their polarization. For enantiomeric pure monolayers of heptahelicene, opposite asymmetries in spin polarization were reported and attributed to the so-called chirality-induced spin selectivity effect. However, these promising proof-of-concept photoemission experiments lack the angular and energy resolution that could provide the necessary insights into the mechanism of this phenomenon. In order to fill in the missing gaps, we provide a detailed spin- and angle-resolved photoemission spectroscopy study of heptahelicene layers on a Cu(111) substrate. Throughout the large accessible energy and angle range, no chirality induced spin asymmetry in photoemission could be observed. Possible reasons for the absence of signatures of the spin-dependent electron transmission through the chiral molecular layer are briefly discussed.

© 2023 Author(s). All article content, except where otherwise noted, is licensed under a Creative Commons Attribution (CC BY) license (<http://creativecommons.org/licenses/by/4.0/>). <https://doi.org/10.1063/5.0156581>

I. INTRODUCTION

Molecular chirality on surfaces has been focus of growing research interest in recent years.^{1–3} Among many molecular classes, helicenes have been of particular interest in this regard. These polycyclic compounds consist of multiple *ortho*-annulated aromatic or heteroaromatic rings that due to a steric hindrance wind to define helicenes' helical structure and chirality. Examples of (*M*)- and (*P*)-heptahelicene ([7]H) molecules are shown in Fig. 1(a). Owing to their helical chirality, they provided insight into chiral crystallization and chiral recognition at surfaces in numerous scanning tunneling

microscopy (STM) experiments.^{4–16} Beside the chiral crystallization and recognition studies, helicenes were of increasing interest in on-surface chemistry^{17–24} and electrochemical sensing and catalysis^{25–27} as well as electron spin filtering aspects.^{28–31} Some of these catalytic or spin filtering effects were explained within the wider Chirality-Induced Spin Selectivity (CISS) effect, standing for spin-dependent transmission of electrons through the layers of chiral molecules.^{32–35} The CISS has drawn significant attention to molecular layers of helical entities on surfaces.

Angle-Resolved Photoemission Spectroscopy (ARPES) has been playing a paramount role in the development of novel

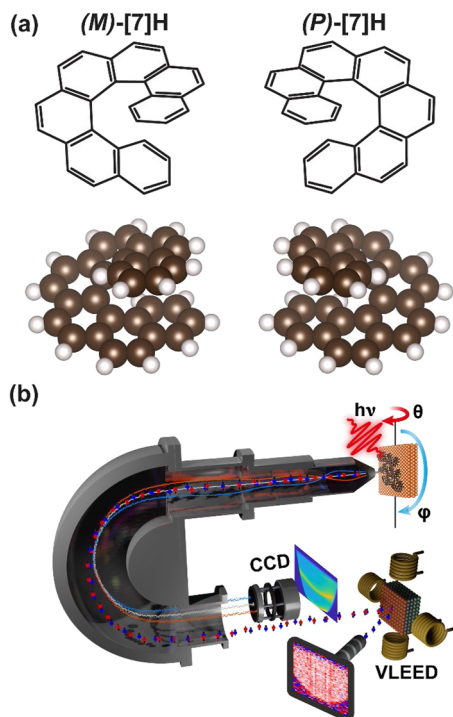


FIG. 1. (a) Molecular structures and ball-and-stick representations of the (*M*)- and (*P*)-[7]H molecules. (b) Experimental setup of the photoemission experiment (see details in Sec. II).

topological and low-dimensional materials.^{36–38} ARPES momentum mapping of the Fermi surface in proximity to the interface represents a powerful tool for investigation of molecule/substrate interfaces as well. As such, it was employed to study changes in the Shockley surface states of Au, Ag, and Cu substrates upon molecular adsorption and their confinement due to the formation of porous molecular networks.^{39–45} Photoemission experiments involving spin detectors have also played their part in the establishment of the aforementioned CISS effect; spin polarizations up to 60% were demonstrated for DNA layers, while polarizations of 6%–8% or up to 24.4% were shown for layers of helicenes and oligopeptides, respectively.^{30,46,47} The effect was also demonstrated for non-helical chiral molecular layers.^{48,49} Albeit these spin-resolved photoemission experiments showed promising results, they lack the angular and/or energy resolution that is necessary to glimpse into the mechanism of this phenomenon.

In this contribution, a detailed angle- and spin-resolved photoemission study of heptahelicene layers on Cu(111) surfaces is presented, attempting to fill in the missing gaps. Experimental setup depiction is shown in Fig. 1(b), while further details are provided in Sec. II of the paper. Our spin-integrated ARPES results demonstrate a sizable but consistent shift of the Shockley surface state of the Cu(111) substrate for all three molecular layers of heptahelicene molecules made, respectively, from racemic, right-handed, and left-handed configuration samples abbreviated (*rac*)-[7]H, (*P*)-[7]H, and (*M*)-[7]H, respectively. At the same time, no difference in the work function in these layers was observed. Our

experimental attempts to energy and/or angle resolve spin polarizations in these layers using an advanced very-low-energy electron diffraction (VLEED) spin detector did not show a difference between the layers consisting of molecules of opposite handedness. Throughout the wide accessible energy and angle range, no difference in spin polarization is observed for the longitudinal (out-of-plane) spin component as well as for the one of the in-plane spin components.

II. EXPERIMENTAL SECTION/METHODS

A. Heptahelicene enantioseparation

Rac-[7]H was purchased from Chiracon GmbH (Luckenwalde, Germany), and separation of enantiomers was performed using high-performance liquid chromatography (HPLC) under semi-preparative conditions. The assignment of absolute handedness to the eluted enantiomers has been performed with UV/VIS circular dichroism. More details about conditions for the separation can be found in the literature.³¹

B. Substrate preparation

The Cu(111) surfaces have been cleaned by repetitive Ar⁺-ion sputtering and annealing. The cleanliness of the substrate was confirmed by UPS spectroscopy using a monochromatic He I α photon source (21.2 eV). *Rac*-, (*P*)-, and (*M*)-[7]H molecules were deposited on substrates kept at room temperature from home-made effusion cells held at 170 °C. A monolayer (ML) coverage was ensured by deposition of an excess of molecules on the surface and subsequent step-wise annealing until no changes were observed in the UPS spectra as shown in Fig. S1 in the supplementary material. A temperature of 65 °C for desorption of layers beyond the first one is consistent with previous studies.^{6,50}

C. Photoemission electron spectroscopy measurements

The angle- (momentum-) and spin-resolved photoemission experiments were conducted with a hemispherical analyzer (SPECS PHOIBOS 150). The analyzer is equipped with a CCD detector system as well as the very-low energy electron diffraction (VLEED) commercial spin detector (Focus FERRUM). The FERRUM spin detector also possesses a spin rotator lens that allows us to record spin-resolved photoemission data for three orthogonal spin components—two spin components parallel to the surface plane (in-plane spin components) and the out-of-plane spin component along the surface normal. The spin sensitivity or Sherman function (*S*) of the detector is 0.29 for all three spin components. Spin polarization curves are plotted with error bars reflecting statistical uncertainties from the count rates in the photoemission experiment. In addition to the monochromatic He I α photon source (21.2 eV), the fourth harmonic of a Ti:sapphire laser oscillator (Tsunami long pulse, Ti:sapphire oscillator system) with a photon energy of 5.9 eV and p-polarized light was used as a photon source. The angle of incidence was 45° with respect to the surface normal for normal emission, and a sample bias of -4 V was applied during the experiments. The laser spot (0.025 cm²) on the sample was defocused, keeping the fluence <0.04 W/cm² to reduce beam induced damage to the molecules. The samples were aligned for a specific azimuthal emission angle (high

symmetry direction of the substrate) and scanned over the polar angle along Γ -M direction. All photoemission spectra are acquired at room temperature.

III. RESULTS AND DISCUSSIONS

A. Angle-resolved spin-integrated photoemission spectroscopy results

Upon the substrate preparation (see details in Sec. II), spin-integrated energy vs momentum cuts around the Γ point are acquired and the results are plotted in Fig. 2. The clean Cu(111) energy vs momentum map shown in Fig. 2(a) contains the typical parabolic dispersion of the Shockley surface state centered at the Γ point, reaching to 0.40 ± 0.01 eV below the Fermi level, well in line with the available literature.^{51–53} On the samples containing 1 ML of heptahelicene molecules, namely, *rac*-[7]H, (*P*)-[7]H, and (*M*)-[7]H [Figs. 2(b)–2(d)], the Shockley surface state of Cu(111) retained its parabolic dispersion around the Γ point, however, it is shifted by 0.16 eV toward the Fermi level in all three cases. Moreover, significant spectral broadening originating from the inelastic scattering from deposited materials is visible. Similar effects are observed upon CO or pentacene adsorption on Cu(111) or Cu(110) substrates, respectively.^{40,51} The presence of heptahelicene molecular monolayers also reduces the work function of the clean Cu(111)

interface by around 1 eV (Fig. S1 in the supplementary material) due to a Pauli repulsion induced charge rearrangement in the substrate (pushback effect).^{31,54–59} The work function reduction, in turn, leads to a new spectroscopic feature often referred to as the Mahan cone. The Mahan cone, visible between -0.8 and -1.2 eV, originates from the direct optical transitions between nearly free-electron *sp*-bands of the Cu(111) substrate and is particularly relevant when an excitation source of around 6 eV, like in our case, is used for the photoemission experiment.^{52,60} Apart from the highly suppressed Shockley surface state, the Mahan cone and the secondary electron cut-off features, no spectral features originating from the Cu 3d states or molecular layers are present. This is further corroborated in the photoemission experiments performed using monochromatic He I α photon source (Fig. S1 in the supplementary material), confirming that the photoemitted electrons mostly originate from the *sp* states of the Cu(111) substrate.

B. Angle- and spin-resolved photoemission spectroscopy results

Following the spin-integrated angle-resolved photoemission experiments, spin-resolved measurements are performed using a VLEED spin detector. The spin polarization was calculated as the normalized difference of the spectral intensities of spin up and spin down electrons using the following equation:

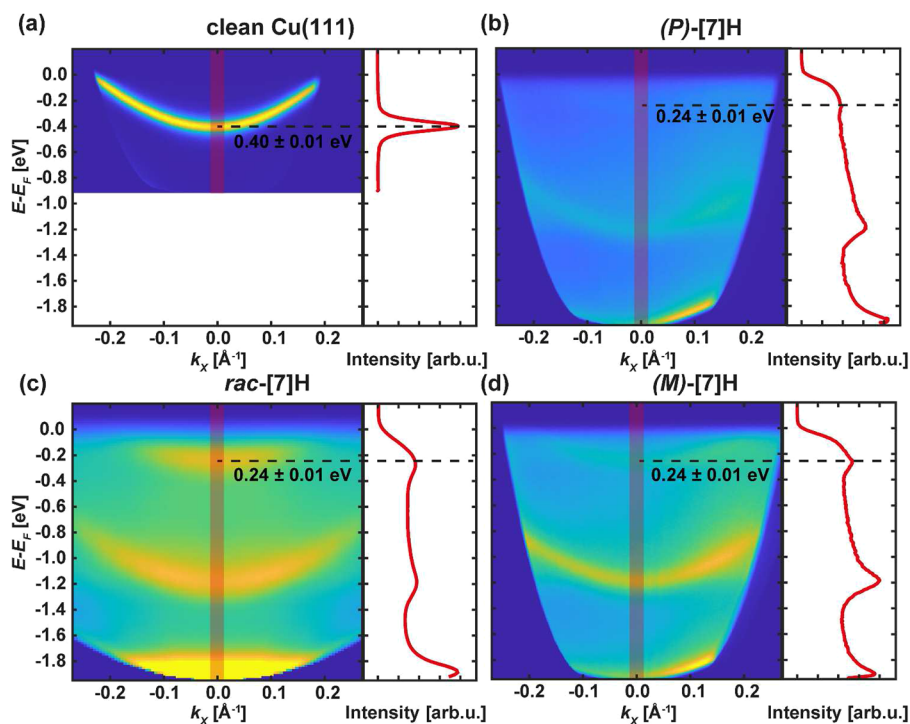


FIG. 2. ARPES k_x momentum maps around the Γ point with momentum cuts at the Γ point shown next to them of a clean Cu(111) substrate (a) and monolayers of (*P*)-[7]H (b), *rac*-[7]H (c), and (*M*)-[7]H (d) molecules on a Cu(111) substrate. Dashed lines indicate the position of the Shockley surface state of the Cu(111) substrate as determined from the momentum cuts at the Γ point (red curves). Highlighted red areas on the map represent area from which the cut at the Γ point is made. A significant but consistent shift of about 0.16 eV is observed for all three molecular layers. Note that the map for *rac*-[7]H is acquired using a VLEED detector while the other three maps are acquired using a CCD detector. All maps are acquired using a laser photon source ($h\nu = 5.9$ eV, p-polarized).

$$P = \frac{I_{\uparrow} - I_{\downarrow}}{I_{\uparrow} + I_{\downarrow}} S^{-1}, \quad (1)$$

with S representing the spin sensitivity or Sherman function.

Detector calibration was checked by the acquisition of spin-resolved spectra of a clean Cu(111) substrate at the Γ point and 12 degrees off the Γ point (Fig. S2 in the supplementary material). No difference in spin polarization is visible for the longitudinal (out-of-plane) spin polarization albeit a small positive offset of polarization is present (Figs. S2a and S2b in the supplementary material). Looking into the in-plane spin polarization, no polarization is present at the Γ point (Fig. S2c in the supplementary material), while the expected polarization flip from positive to negative values originating from the Rashba split Shockley surface state is observed in the spectra acquired 12° off the Γ point (Fig. S2d in the supplementary material).⁵³ The energy averages of spin polarizations plotted in Fig. S2 are shown in Table SI in the supplementary material.

First, spin-resolved spectra of *rac*-, (*P*)-, and (*M*)-heptahelicene monolayers on Cu(111) are acquired at the Γ point and corresponding out-of-plane spin polarizations are calculated using Eq. (1). The results are summarized in Fig. S3 in the supplementary material. The spectra fully resemble those acquired using the spin-integrated detector with the surface state, the Mahan cone, and the secondary electron cut-off feature. Interestingly, for all three molecular monolayers of different enantiomeric compositions, namely, *rac*-, (*P*)-, and (*M*)-[7]H, similar spin polarization curves are observed. In all the cases, a slight positive net spin polarization is observed. The polarization is of similar magnitude as observed on the clean

Cu(111) during the calibration check (Fig. S2a in the supplementary material). Moreover, a similar spin polarization is observed in the spectra acquired at the Γ point of a multilayer of (*M*)-[7]H on Cu(111) using a laser photon source (Fig. S4a in the supplementary material) and in the spectra acquired at the Γ point of a monolayer of (*M*)-[7]H on Cu(111) using a monochromatic He I α photon source (Fig. S4b in the supplementary material). This is a surprising result, given that the previous results on photoemission experiments with the same molecules on Cu(332), Au(111), and Ag(110) substrates were showing out-of-plane spin polarizations of around $\pm 7\%$ for (*P*)- and (*M*)-[7]H in the normal incidence–normal emission setup.³⁰

Next, angle- and spin-resolved maps of the same monolayers were acquired by varying the polar angle to around 32 degrees off sample normal. Total intensity maps, constructed as sums of spin up and spin down photoelectron intensities, corresponding spin polarization maps constructed by applying Eq. (1) to every point/angle, and angle averaged spin polarizations for monolayers of (*P*)-, *rac*-, and (*M*)-[7]H molecules on Cu(111) are shown in Figs. 3(a)–3(c), respectively. Upon the map acquisitions, samples were checked for potential beam induced damage to molecular layers. This was performed by comparing VUV spin-integrated spectra of a monolayer of (*P*)-[7]H molecules on the Cu(111) substrate before and after the acquisition of spin-resolved map (Fig. S5 in the supplementary material). No changes in the spectra are observed, indicating that no beam induced damage occurred during the time required to acquire spin-resolved maps.

The total intensity maps, shown in the top panels of Fig. 3, resemble the spin-integrated maps from Fig. 2—upward shifted

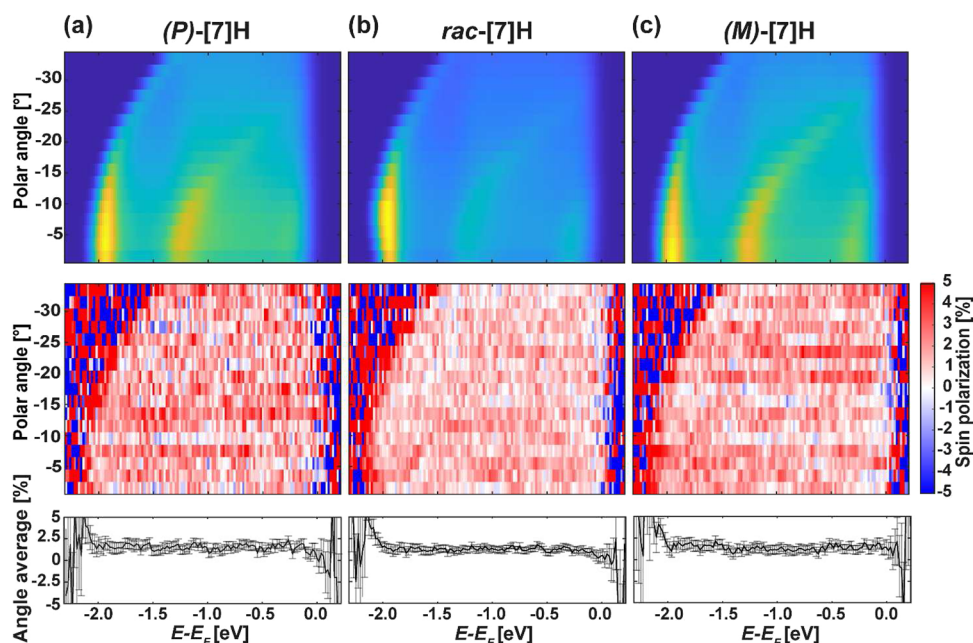


FIG. 3. Angle-resolved photoemission experiment using a VLEED spin detector. Angle-resolved spin sum maps (top), out-of-plane spin polarization maps (middle), and angle averaged spin polarizations (bottom) of monolayers of (a) (*P*)-[7]H, (b) *rac*-[7]H, and (c) (*M*)-[7]H molecules on the Cu(111) substrate. Spin polarization was calculated using Eq. (1). All maps were acquired using a laser photon source ($h\nu = 5.9$ eV, p-polarized).

Shockley surface states of Cu(111), the Mahan cone, and secondary electron cut-off features are clearly visible. The spin-resolved maps, shown in the middle panels of Fig. 3, look very similar for all three molecular chiralities. In all the maps, slight positive spin-polarization is present well in line with the results shown in Figs. S2 and S3 in the supplementary material. These become even more apparent looking at the bottom panels of Fig. 3, where the angle averaged spin polarizations for all three molecular layers are shown. Further to this, performing energy averaging onto these angle averaged spin polarization plots results in the total raw spin polarizations of around $1.25\% \pm 0.03\%$ if averaging is performed over energies above -1.26 eV, $1.28\% \pm 0.06\%$ if performed from -2.0 eV, and $1.4\% \pm 0.3\%$ if it is performed over the whole energy range for all three layers. Exact values for each energy range and molecular chirality, not corrected to the spin polarizations of bare Cu(111), are summarized in Table SI in the supplementary material. The difference in values arises due to the interdependences of the available energy range for different polar angles, thus resulting in lower statistics in the region beyond -1.26 eV. The -1.26 eV value was set as a limit for averaging for several reasons: first, spectroscopic data are available for all measured polar angles down to this energy, which is essential for a better statistics in the averaged plot. Second, the Mahan cone is present in this energy range. Last, due to a higher work function of the heptahelicene/Cu(332) interface, this was the region that was reachable in the previous photoemission experiment,³⁰ making a comparison to the same energy ranges easier.

Finally, we have studied one of the in-plane spin-polarization components for (P) -[7]H and rac -[7]H molecular monolayers on Cu(111). These maps are shown in Fig. 4. Both maps show a small negative spin-polarization that coincides with the one of the calibration sample shown in Fig. S2 of the supplementary material. However, no apparent difference related to molecular chirality is observed.

The natural question that arises from our study is the possible reason for the absence of spin-polarization in our experiments, in particular since the other photoemission studies have reported sizable longitudinal spin-polarizations for similar metal-molecule interfaces. The first option of the experimental error seems unlikely—experiments in this comprehensive study were performed with great care, and samples were checked for beam damage; the energy and polar angle steps were chosen within the experimental limitations of the experimental setup but taking into account the acceptance angle of the analyzer for the -4 V bias that was applied between the sample and the analyzer to ensure there are no missing data in the acquired steps. Similarly, the laser was defocused and dwell time was optimized to avoid beam damage of the molecular films but still providing sufficient counts for high signal to noise ratio. The longitudinal (out-of-plane) spin was probed throughout most of the paper since it has been shown that it is the preferential spin filtering direction for helical moieties.^{30,46,49} Spin polarization maps presented in Fig. 4 also show the absence of spin polarization in one of the in-plane components albeit focus was on detailed investigation of the out-of-plane spin component.

At low temperatures, adsorbed heptahelicene molecules on the Cu(111) substrate exhibit six different azimuthal orientations,^{6,12,61} however, that should not have an influence on the results shown herein that are acquired at room temperature where molecules

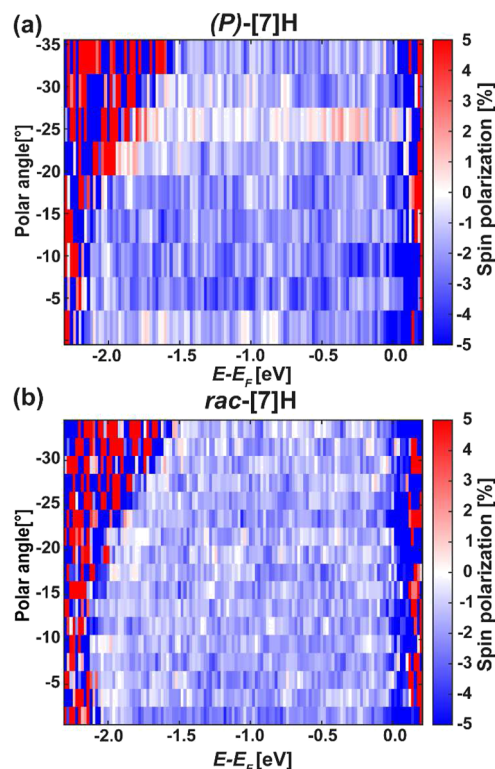


FIG. 4. In-plane spin polarization maps of monolayers of (a) (P) -[7]H and (b) rac -[7]H molecules on the Cu(111) substrate. Spin polarization was calculated using Eq. (1). Maps are acquired using a laser photon source ($h\nu = 5.9$ eV, p-polarized).

should still exhibit significant mobility. This would just mean that we are probing an average ensemble of heptahelicene molecules with different azimuthal orientations. Moreover, similar structural motifs are found for heptahelicene molecules on Ag(111) and Au(111) substrates⁵ of which Au(111) was included in the previous photoemission study performed at room temperature.³⁰ The presence of chirality dependent spin polarizations in their experiment on the Au(111) substrate suggests that the azimuthal orientation of heptahelicene molecules cannot be the origin of its absence in this study.

Next, the work function differences of the heptahelicene/Cu interfaces for surfaces with different crystallographic orientations have to be considered. For monolayers of heptahelicene molecules on Cu(111) and Cu(100), the work function is around 4 eV, while the 4.65 eV work function on the Cu(332) substrate is clearly larger.^{30,31} A smaller work function as detected in our case leads only to a larger accessible kinetic energy range of the emitted photoelectrons and could affect the spin-dependent electron transmission through the molecular layer. Noteworthy, no additional molecular or d-states of the Cu substrate are probed within the extended energy range, as was discussed earlier. Moreover, averaging performed to the comparable energy range to the one accessible on the Cu(332) substrate shows no difference in spin polarization for heptahelicene.

The angle of incidence of incoming photons is the first apparent difference when comparing our experimental setups with the one used by Kettner *et al.*³⁰ Despite the fact that both experiments use laser light of around 5.9 eV as a photon source, the experiments reported in Ref. 30 were conducted in normal incidence geometry while we use an incidence angle around 45 degrees off sample normal. However, this is unlikely to cause this discrepancy, given the variety of geometries employed in ARPES experiments.^{36–38} Moreover, Kettner *et al.* also investigated heptahelicene molecules on Cu(332) substrates, where molecules adsorb with a tilt with respect to the sample normal of around 10°,⁶¹ emulating the non-normal light incidence orientation. The hypothesis that the angle of photon incidence cannot be the reason for the absence of chirality dependent spin polarization in this study is further corroborated in a recent publication where the same setup with 45° light incidence was used to fully vectorially resolve spin polarization originating from the all-chiral metal–molecule heterostructure consisting of point-chiral 3-methylcyclohexanone molecules adsorbed on Cu(643)^R substrates.⁴⁹ The same applies when the light polarization is considered—Kettner *et al.* demonstrated comparable spin polarizations with different light polarizations, and the aforementioned experiment with 3-methylcyclohexanone molecules was employing same light polarization as in this study.

A significant difference between the two experiments lies in the sample preparation procedure. In this work, molecules were deposited on substrates kept at room temperature from effusion cells held at 170 °C and monolayer coverage was ensured by desorption of excess molecules by annealing to 65 °C. This temperature was determined through stepwise annealing until no changes due to a molecular desorption were observed in the UPS spectra. A previous study showed that a closed-packed monolayer of (*M*)-[7]H is formed under such conditions.⁶ Potential heptahelicene dehydrogenation or a Diels–Alder type cycloaddition can be excluded here as it occurs at temperatures of 250–300 °C.^{18,22,50} In the previous work of Kettner *et al.*, heptahelicene molecules were sublimed from an effusion cell held at 160 °C onto substrates kept at a temperature of 200 °C,³⁰ which is still lower than the temperatures for first layer desorption or dehydrogenation. It is unclear if such different preparation conditions would affect molecular packing or the CISS effect.

The last striking difference we are aware of is the applied bias between the samples and an analyzer. In this study, we have applied a 4 V bias, which is typical for photoemission experiments and should have almost no effect on the interface and angular resolution.⁵² In the previous photoemission study of Kettner *et al.*, most likely a larger bias voltage was applied. However, a comparison of typical sample-analyzer distances (few centimeters) with the thickness of a helicene monolayer (few Å) leads us to the conclusion that the difference in voltage drop over the [7]H/Cu(111) is negligible.

All of this lead us to the conclusion that either the different sample preparation procedures or the high bias enables the CISS effect through some unidentified mechanism and is the reason for its absence in our experiments. Nevertheless, it is clear that there is no signature of CISS in the here investigated samples of heptahelicene layers on Cu(111) substrates. The herein investigated interfaces were not part of the previous studies, leaving these possibilities equally probable.

IV. CONCLUSION

In this contribution, detailed angle- and spin-resolved photoemission study of heptahelicene layers on Cu(111) surfaces is presented, attempting to tackle the mechanism of the chirality induced spin selectivity effect. Our spin-integrated results demonstrate a work function change of about 1 eV upon molecular adsorption for all the investigated molecular chiralities. At the same time, consistent upward shifts of the Shockley surface states originating from the Pauli repulsion induced charge rearrangement in the substrate were observed and were accompanied by significant spectral broadening originating from inelastic scattering on the molecular layers.

Our spin-resolved results reveal no differences in spin-polarizations over large angle and energy ranges regardless of the molecular chirality for the preferential out-of-plane but also in-plane spins. This is in contrast with the previous photoemission experiments dealing with the CISS effect, and differences between these experiments are discussed in an attempt to identify the origin of the absence of the CISS effect in our experiments. It has led us to the conclusion that either a difference in sample preparation or the unusually high bias employed in the previous experiments enables the CISS effect through an unknown mechanism or there is no CISS in the here investigated systems of heptahelicene layers on Cu(111) substrates.

SUPPLEMENTARY MATERIAL

See the supplementary material for Figs. S1–S5 and Tables SI–SII that include information about the sample preparation (Fig. S1), spin detector calibration check (Fig. S2 and Table SI), spin-resolved photoemission spectra with corresponding spin polarizations of molecular monolayers on Cu(111) at the Γ point acquired using a laser photon source (Fig. S3), spin-resolved photoemission spectra at the Γ point with corresponding spin polarizations of a multilayer of (*M*)-[7]H on Cu(111) acquired using a laser photon source and a monolayer of (*M*)-[7]H on Cu(111) acquired using a VUV photon source (Fig. S4), VUV spin-integrated photoemission spectra used to assess beam damage (Fig. S5), and tabular representation of angle and energy averaged spin polarizations for different molecular layers and energy ranges (Table SII).

ACKNOWLEDGMENTS

The experimental work was supported from the Swiss National Science Foundation (Grant Nos. CRII5_173720 and 182082) and the University of Geneva as well as by the Deutsche Forschungsgemeinschaft (DFG, German Research Foundation), TRR No. 173-268565370 Spin + X: spin in its collective environment (Project No. B05/B14). B.S. acknowledges financial support by the Dynamics and Topology Center funded by the State of Rhineland Palatinate. Authors thank Professor Helmut Zacharias and Professor Hugo Dil for the fruitful discussions. ChatGPT was used to aid authors correct text to the use of definite/indefinite articles.

AUTHOR DECLARATIONS

Conflict of Interest

The authors have no conflicts to disclose.

Author Contributions

M. Baljović: Conceptualization (equal); Data curation (equal); Formal analysis (equal); Investigation (equal); Visualization (equal); Writing – original draft (lead); Writing – review & editing (equal). **B. Arnoldi:** Data curation (equal); Formal analysis (equal); Investigation (equal); Resources (supporting); Supervision (supporting); Writing – review & editing (equal). **S. Grass:** Resources (supporting); Writing – review & editing (equal). **J. Lacour:** Resources (supporting); Supervision (supporting); Writing – review & editing (equal). **M. Aeschlimann:** Conceptualization (equal); Funding acquisition (equal); Project administration (equal); Resources (supporting); Supervision (supporting); Writing – review & editing (equal). **B. Stadtmüller:** Conceptualization (equal); Data curation (equal); Formal analysis (equal); Funding acquisition (equal); Investigation (equal); Project administration (equal); Resources (supporting); Supervision (supporting); Writing – review & editing (equal). **K.-H. Ernst:** Conceptualization (equal); Data curation (equal); Formal analysis (equal); Funding acquisition (equal); Investigation (equal); Project administration (equal); Resources (equal); Supervision (equal); Writing – review & editing (equal).

DATA AVAILABILITY

The data that support the findings of this study are available within the article and its supplementary material.

REFERENCES

- 1 K.-H. Ernst, *Surf. Sci.* **613**, 1–5 (2013).
- 2 K.-H. Ernst, in *Supramolecular Chirality*, edited by M. Crego-Calama and D. N. Reinhoudt (Springer, Berlin, Heidelberg, 2006), pp. 209–252.
- 3 F. Zaera, *Chem. Soc. Rev.* **46**(23), 7374–7398 (2017).
- 4 K.-H. Ernst, *Acc. Chem. Res.* **49**(6), 1182–1190 (2016).
- 5 J. Seibel, M. Parschau, and K.-H. Ernst, *J. Phys. Chem. C* **118**(50), 29135–29141 (2014).
- 6 K.-H. Ernst, M. Parschau, and R. Fasel, *e-J. Surf. Sci. Nanotechnol.* **2**, 136–140 (2004).
- 7 M. Parschau, R. Fasel, and K.-H. Ernst, *Cryst. Growth Des.* **8**(6), 1890–1896 (2008).
- 8 B. Irziqat, J. Berger, J. I. Mendieta-Moreno, M. S. Sundar, A. V. Bedekar, and K.-H. Ernst, *ChemPhysChem* **22**(3), 293–297 (2021).
- 9 C. M. Hauke, P. Rahe, M. Nimmrich, J. Schütte, M. Kittelmann, I. G. Stará, I. Starý, J. Rybáček, and A. Kühnle, *J. Phys. Chem. C* **116**(7), 4637–4641 (2012).
- 10 M. Stöhr, S. Boz, M. Schär, M.-T. Nguyen, C. A. Pignedoli, D. Passerone, W. B. Schweizer, C. Thilgen, T. A. Jung, and F. Diederich, *Angew. Chem., Int. Ed.* **50**(42), 9982–9986 (2011).
- 11 H. Ascolani, M. W. van der Meijden, L. J. Cristina, J. E. Gayone, R. M. Kellogg, J. D. Fuhr, and M. Lingenfelder, *Chem. Commun.* **50**(90), 13907–13909 (2014).
- 12 R. Fasel, M. Parschau, and K.-H. Ernst, *Angew. Chem., Int. Ed.* **42**(42), 5178–5181 (2003).
- 13 V. Stetsovych, S. Feigl, R. Vranik, B. Wit, E. Rauls, J. Nejedlý, M. Šámal, I. Starý, and S. Müllberger, *Sci. Rep.* **12**(1), 2865 (2022).
- 14 B. C. Baciú, T. de Ara, C. Sabater, C. Untiedt, and A. Guijarro, *Nanoscale Adv* **2**(5), 1921–1926 (2020).
- 15 H. Zhang, H. Liu, C. Shen, F. Gan, X. Su, H. Qiu, B. Yang, and P. Yu, *Int. J. Mol. Sci.* **20**(8), 2018 (2019).
- 16 H. Cao, A. Minoia, I. D. De Cat, J. Seibel, D. Waghay, Z. Li, D. Cornil, K. S. Mali, R. Lazzaroni, W. Dehaen, and S. D. De Feyter, *Nanoscale* **9**(45), 18075–18080 (2017).
- 17 A. Mairena, C. Wäckerlin, M. Wienke, K. Grenader, A. Terfort, and K.-H. Ernst, *J. Am. Chem. Soc.* **140**(45), 15186–15189 (2018).
- 18 A. Mairena, M. Baljović, M. Kawecki, K. Grenader, M. Wienke, K. Martin, L. Bernard, N. Avarvari, A. Terfort, K.-H. Ernst, and C. Wäckerlin, *Chem. Sci.* **10**(10), 2998–3004 (2019).
- 19 J. Voigt, M. Roy, M. Baljović, C. Wäckerlin, Y. Coquerel, M. Gingras, and K.-H. Ernst, *Chem. Eur J.* **27**(40), 10251–10254 (2021).
- 20 B. Irziqat, A. Cebrat, M. Baljović, K. Martin, M. Parschau, N. Avarvari, and K.-H. Ernst, *Chem. Eur J.* **27**(54), 13523–13526 (2021).
- 21 A. Shchyrba, M.-T. Nguyen, C. Wäckerlin, S. Martens, S. Nowakowska, T. Ivas, J. Roose, T. Nijs, S. Boz, M. Schär, M. Stöhr, C. A. Pignedoli, C. Thilgen, F. Diederich, D. Passerone, and T. A. Jung, *J. Am. Chem. Soc.* **135**(41), 15270–15273 (2013).
- 22 O. Stetsovych, M. Švec, J. Vacek, J. V. Chocholoušová, A. Jančařík, J. Rybáček, K. Kosmider, I. G. Stará, P. Jelínek, and I. Starý, *Nat. Chem.* **9**(3), 213–218 (2017).
- 23 R. Zuzak, J. Castro-Esteban, P. Brandimarte, M. Engelund, A. Cobas, P. Piątkowski, M. Kolmer, D. Pérez, E. Guitián, M. Szymonski, D. Sánchez-Portal, S. Godlewski, and D. Peña, *Chem. Commun.* **54**(73), 10256–10259 (2018).
- 24 J. Li, K. Martin, N. Avarvari, C. Wäckerlin, and K.-H. Ernst, *Chem. Commun.* **54**(57), 7948–7951 (2018).
- 25 M. Tounsi, M. Ben Braiek, A. Baraket, M. Lee, N. Zine, M. Zabala, J. Bausells, F. Aloui, B. Ben Hassine, A. Maaref, and A. Errachid, *Electroanalysis* **28**(12), 2892–2899 (2016).
- 26 Y. Liang, K. Banjac, K. Martin, N. Zigon, S. Lee, N. Vanthuyne, F. A. Garcés Pineda, J. Galan-Mascaros, X. Hu, N. Avarvari, and M. Lingenfelder, *Nat. Commun.* **13**, 3356 (2022).
- 27 D. Dova, L. Viglianti, P. R. Mussini, S. Prager, A. Dreuw, A. Voituriez, E. Licandro, and S. Cauteruccio, *Asian J. Org. Chem.* **5**(4), 537–549 (2016).
- 28 V. Kiran, S. P. Mathew, S. R. Cohen, I. H. Hernández Delgado, J. Lacour, and R. Naaman, *Adv. Mater.* **28**(10), 1957–1962 (2016).
- 29 T.-R. Pan, A.-M. Guo, and Q.-F. Sun, *Phys. Rev. B* **94**(23), 235448 (2016).
- 30 M. Kettner, V. V. Maslyuk, D. Nürenberg, J. Seibel, R. Gutierrez, G. Cuniberti, K.-H. Ernst, and H. Zacharias, *J. Phys. Chem. Lett.* **9**(8), 2025–2030 (2018).
- 31 M. Baljović, A. L. Fernandes Cauduro, J. Seibel, A. Mairena, S. Grass, J. Lacour, A. K. Schmid, and K.-H. Ernst, *Phys. Status Solidi B* **258**(12), 2100263 (2021).
- 32 R. Naaman and D. H. Waldeck, *J. Phys. Chem. Lett.* **3**(16), 2178–2187 (2012).
- 33 R. Naaman, Y. Paltiel, and D. H. Waldeck, *J. Phys. Chem. Lett.* **11**(9), 3660–3666 (2020).
- 34 C. D. Aiello, J. M. Abendroth, M. Abbas, A. Afanasev, S. Agarwal, A. S. Banerjee, D. N. Beratan, J. N. Belling, B. Berche, A. Botana, J. R. Caram, G. L. Celardo, G. Cuniberti, A. Garcia-Etxarri, A. Dianat, I. Diez-Perez, Y. Guo, R. Gutierrez, C. Herrmann, J. Hihath, S. Kale, P. Kurian, Y.-C. Lai, T. Liu, A. Lopez, E. Medina, V. Mujica, R. Naaman, M. Noormandipour, J. L. Palma, Y. Paltiel, W. Petuskey, J. C. Ribeiro-Silva, J. J. Saenz, E. J. G. Santos, M. Solyanik-Gorgone, V. J. Sorger, D. M. Stemer, J. M. Ugalde, A. Valdes-Curiel, S. Varela, D. H. Waldeck, M. R. Wasielewski, P. S. Weiss, H. Zacharias, and Q. H. Wang, *ACS Nano* **16**(4), 4989–5035 (2022).
- 35 F. Evers, A. Aharony, N. Bar-Gill, O. Entin-Wohlman, P. Hedegård, O. Hod, P. Jelínek, G. Kamieniarz, M. Lemesshko, K. Michaeli, V. Mujica, R. Naaman, Y. Paltiel, S. Refaely-Abramson, O. Tal, J. Thijssen, M. Thoss, J. M. van Ruitenbeek, L. Venkataraman, D. H. Waldeck, B. Yan, and L. Kronik, *Adv. Mater.* **34**(13), 2106629 (2022).
- 36 A. A. Kordyuk, *Low Temp. Phys.* **40**(4), 286–296 (2014).
- 37 S.-K. Mo, *Nano Converg* **4**(1), 6 (2017).
- 38 Y. Chen, X. Gu, Y. Li, X. Du, L. Yang, and Y. Chen, *Matter* **3**(4), 1114–1141 (2020).
- 39 J. Lobo-Checa, M. Matena, K. Müller, J. H. Dil, F. Meier, L. H. Gade, T. A. Jung, and M. Stöhr, *Science* **325**(5938), 300–303 (2009).
- 40 A. Scheybal, K. Müller, R. Bertschinger, M. Wahl, A. Bendounan, P. Aebi, and T. A. Jung, *Phys. Rev. B* **79**(11), 115406 (2009).
- 41 S. Nowakowska, F. Mazzola, M. N. Alberti, F. Song, T. Voigt, J. Nowakowski, A. Wäckerlin, C. Wäckerlin, J. Wiss, W. B. Schweizer, M. Broszio, C. Polley, M. Leandersson, S. Fatayer, T. Ivas, M. Baljović, S. F. Mousavi, A. Ahsan, T. Nijs, O. Popova, J. Zhang, M. Muntwiler, C. Thilgen, M. Stöhr, I. A. Pasti, N. V.

- Skorodumova, F. Diederich, J. Wells, and T. A. Jung, *ACS Nano* **12**(1), 768–778 (2018).
- ⁴²M. Baljović, X. Liu, O. Popova, J. Girovsky, J. Nowakowski, H. Rossmann, T. Nijs, M. Moradi, S. F. Mousavi, N. C. Plumb, M. Radović, N. Ballav, J. Dreiser, S. Decurtins, I. A. Pašti, N. V. Skorodumova, S.-X. Liu, and T. A. Jung, *Magnetochemistry* **7**(8), 119 (2021).
- ⁴³R. Nemoto, P. Krüger, A. N. Putri Hartini, T. Hosokai, M. Horie, S. Kera, and T. K. Yamada, *J. Phys. Chem. C* **123**(31), 18939–18950 (2019).
- ⁴⁴C.-S. Zhou, X.-R. Liu, Y. Feng, X. Shao, M. Zeng, K. Wang, M. Feng, and C. Liu, *Appl. Phys. Lett.* **117**(19), 191601 (2020).
- ⁴⁵I. Piquero-Zulaica, S. Nowakowska, J. E. Ortega, M. Stöhr, L. H. Gade, T. A. Jung, and J. Lobo-Checa, *Appl. Surf. Sci.* **391**, 39–43 (2017).
- ⁴⁶B. Göhler, V. Hamelbeck, T. Z. Markus, M. Kettner, G. F. Hanne, Z. Vager, R. Naaman, and H. Zacharias, *Science* **331**(6019), 894–897 (2011).
- ⁴⁷P. V. Möllers, S. Ulku, D. Jayarathna, F. Tassinari, D. Nürenberg, R. Naaman, C. Achim, and H. Zacharias, *Chirality* **33**(2), 93–102 (2021).
- ⁴⁸M. Á. Niño, I. A. Kowalik, F. J. Luque, D. Arvanitis, R. Miranda, and J. J. de Miguel, *Adv. Mater.* **26**(44), 7474–7479 (2014).
- ⁴⁹C. Badala Viswanatha, J. Stöckl, B. Arnoldi, S. Becker, M. Aeschlimann, and B. Stadtmüller, *J. Phys. Chem. Lett.* **13**(26), 6244–6249 (2022).
- ⁵⁰K.-H. Ernst, Y. Kuster, R. Fasel, M. Müller, and U. Ellerbeck, *Chirality* **13**(10), 675–678 (2001).
- ⁵¹F. Baumberger, T. Greber, B. Delley, and J. Osterwalder, *Phys. Rev. Lett.* **88**(23), 237601 (2002).
- ⁵²M. Hengsberger, F. Baumberger, H. J. Neff, T. Greber, and J. Osterwalder, *Phys. Rev. B* **77**(8), 085425 (2008).
- ⁵³A. Tamai, W. Meevasana, P. D. C. King, C. Nicholson, A. de la Torre, E. Rozbicki, and F. Baumberger, *Phys. Rev. B* **87**(7), 075113 (2013).
- ⁵⁴G. Witte, S. Lukas, P. S. Bagus, and C. Wöll, *Appl. Phys. Lett.* **87**(26), 263502 (2005).
- ⁵⁵P. S. Bagus, K. Hermann, and C. Wöll, *J. Chem. Phys.* **123**(18), 184109 (2005).
- ⁵⁶R. Caputo, B. P. Prascher, V. Staemmler, P. S. Bagus, and C. Wöll, *J. Phys. Chem. A* **111**(49), 12778–12784 (2007).
- ⁵⁷T. Bauert, L. Zoppi, G. Koller, A. Garcia, K. K. Baldrige, and K.-H. Ernst, *J. Phys. Chem. Lett.* **2**(21), 2805–2809 (2011).
- ⁵⁸A. Mairena, L. Zoppi, S. Lampart, K. K. Baldrige, J. S. Siegel, and K. Ernst, *Chem. Eur. J.* **25**(49), 11555–11559 (2019).
- ⁵⁹L. Zoppi, Q. Stöckl, A. Mairena, O. Allemann, J. S. Siegel, K. K. Baldrige, and K.-H. Ernst, *J. Phys. Chem. B* **122**(2), 871–877 (2018).
- ⁶⁰A. Winkelmann, A. A. Akin Ünal, C. Tusche, M. Ellguth, C.-T. Chiang, and J. Kirschner, *New J. Phys.* **14**(8), 083027 (2012).
- ⁶¹R. Fasel, A. Cossy, K.-H. Ernst, F. Baumberger, T. Greber, and J. Osterwalder, *J. Chem. Phys.* **115**(2), 1020–1027 (2001).